NASA Technical Memorandum 100563

AN APPLICATION OF ACTIVE SURFACE HEATING FOR AUGMENTING LIFT AND REDUCING DRAG OF AN AIRFOIL

(NASA-TM-100563) AN APPLICATION OF ACTIVE SURFACE HEATING FOR AUGMENTING LIFT AND REDUCING DRAG OF AN AIRFOIL (NASA) 17 p CSCL 01A

N88-16570

Unclas
G3/02 0129989

Lucio Maestrello

Forooz F. Badavi

Kevin W. Noonan

MARCH 1988

National Aeronautics and Space Administration

Langley Research Center
Hampton, Virginia 23665-5225

ABSTRACT

Application of active control to separated flow on the RC(6)-08 airfoil at high angle of attack by localized surface heating is numerically simulated by integrating the compressible two-dimensional nonlinear Navier-Stokes equations solver. Active control is simulated by local modification of the temperature boundary condition over a narrow strip on the upper surface of the airfoil. Both mean and perturbed profiles are favorably altered when excited with the same natural frequency of the shear layer by moderate surface heating for both laminar and turbulent separation. The shear layer is found to be very sensitive to localized surface heating in the vicinity of the separation point. The excitation field at the surface sufficiently altered both the local as well as the global circulation to cause a significant increase in lift and reduction in drag.

INTRODUCTION

The first known effort on the use of boundary layer control for reducing drag in the U.S.A. was made by NACA at the Langley Laboratory in the Low Turbulence Pressure Tunnel (LTPT) in 1939. In 1941, NACA conducted what is believed to be the first laminar suction experiment. This was reported in an unpublished paper by Maskell and described by Flatt[1] in 1961. This effort was apparently triggered by the results of contemporary German work, later reported by Holstein[2].

In recent years, the application of boundary layer control has been divided into high lift and low drag. The first deals with separation control and the second with laminar flow control and turbulent manipulation[3-15].

Design constraints between high speed cruise and low speed take-off and landing has forced the designers of fixed wing aircraft to incorporate some form of high lift device to improve lift at low speed. The improvements have been accommodated within the configuration of the trailing edge flap and leading edge slat.

In rotary wing aircraft additional constraints exist[16]. In flight, the rotor blade is exposed cyclically to different flow about the azimuthal position in the rotational disk. The blade advancing into the oncoming airstream experiences high dynamic pressure and needs only small angles of attack to produce adequate lift to maintain roll trim. At the opposite side of the disk, the retreating blade experiences low dynamic pressure and therefore operates at high angles of attack to develop an adequate lift. When the airfoil reaches high angles of attack, the generated flow field can be characterized by massive unsteady separation originating near the leading edge and by large scale vortical structures. Within this complex flow, one encounters the phenomenon of dynamic stall, a behavior dominated by the dynamic stall vortex.

Several investigators have developed analytical models for rotor flow[17]. Most cases provide a solution to the full potential equation. An important design consideration for the rotor and the blades is to operate at high lift conditions. Ideally, in this situation, the boundary layer must not separate. However, if the angle of attack is increased sufficiently, separation is unavoidable. Using flow control techniques, a number of benefits can be envisioned to control separation. One of these is to improve lift and stall characteristics. Applications of active control both in the laboratory[6,7] and in numerical experiments[8-10] have been performed successfully.

In this paper, the steady and unsteady flow about the RC(6)-08 rotor airfoil relevant to the issue of dynamic stall and its origins and the method of controlling it by active means is investigated. In the simulation, the full two-dimensional compressible Navier-Stokes equations solver developed by Rumsey and Anderson and Rumsey and Thomas[18,19] is used and the control is by surface heating. Their work successfully predicted lift and stall angle for airfoils. The flow being investigated is characterized by the shedding of a strong vortex from the leading edge. The viscous layer is of the order of the airfoil chord during the vortex shedding process. This class of flow problems may properly be simulated only by use of the full Navier-Stokes equations.

The results presented herein contains both steady and unsteady data including lift and drag coefficients at Reynolds numbers (based on chord) Re of 10^5 and 3×10^5 for laminar simulation and 5.2×10^6 for turbulent simulation. The objective is to investigate the active control of disturbances in the boundary layer by localized surface heating. The concern is with the nature of the interaction of the time dependent disturbance in a separated boundary layer and the ability to actively perturb the layer to reduce and prevent separation. It is shown that control of separated flow can be successfully achieved using localized active surface heating.

NUMERICAL METHOD

The solution of the compressible two-dimensional Navier-Stokes equations is used to compute the laminar flow and a suitable turbulent modeling is used to compute the turbulent flow about the RC(6)-08 airfoil. The method is an upwind-biased implicit approximate factorization Navier-Stokes algorithm described by Rumsey and Anderson[18] and Rumsey and Thomas.[19] The complete form of the two-dimensional compressible Navier-Stokes equations (at low Reynolds number for laminar flow and high Reynolds number for turbulent flow) are evaluated. The equations are written in generalized coordinates and conservation form:

$$\frac{\partial \hat{Q}}{\partial t} + \frac{\partial \hat{G}}{\partial \eta} + \frac{\partial \hat{H}}{\partial \zeta} = \bar{R}e^{-1} \{\partial_\eta[J^{-1}(\eta_x R + \eta_y S)] + \partial_\zeta[J^{-1}(\zeta_x R + \zeta_y S)]\} \tag{1}$$

$$\hat{Q} = Q/J$$

$$\hat{G} = (\eta_x G + \eta_y H)/J \tag{2}$$

$$\hat{H} = (\zeta_x G + \zeta_y H)/J$$

$$Q = \begin{bmatrix} \rho \\ \rho u \\ \rho v \\ e \end{bmatrix} \qquad G = \begin{bmatrix} \rho u \\ \rho u^2+p \\ \rho uv \\ u(e+p) \end{bmatrix} \qquad H = \begin{bmatrix} \rho v \\ \rho uv \\ \rho v^2+p \\ v(e+p) \end{bmatrix} \tag{3}$$

$$p = (\gamma-1)[e-0.5\rho(u^2 + v^2)] \tag{4}$$

where η is the coordinate along the body, ζ is the coordinate normal to the body, ρ is the density, u and v are the x and y components of velocities, and e is the total energy.

The viscous terms on the right hand side are given by

$$R = \begin{bmatrix} 0 \\ \tau_{xx} \\ \tau_{xy} \\ R_4 \end{bmatrix} \qquad S = \begin{bmatrix} 0 \\ \tau_{xy} \\ \tau_{yy} \\ S_4 \end{bmatrix} \tag{5}$$

All viscous terms are centrally differenced and implicit cross-derivative terms are neglected in the formulation. This algorithm is accurate to the first order in time and second in space. Implicit spatial derivatives of the convection and pressure terms are first order accurate. For turbulent calculations, the two layer algebraic eddy viscosity model of Baldwin and Lomax[20] is employed.

Boundary conditions are applied explicitly. No slip, adiabatic wall conditions, as well as zero pressure conditions are applied on the body:

$$u = v = 0$$

$$\frac{\partial p}{\partial \zeta} = \frac{\partial a^2}{\partial \zeta} = 0 \qquad (6)$$

where a^2 is proportional to the temperature and a is the speed of sound. In the farfield, the subsonic freestream boundary conditions are determined through a characteristic analysis normal to the body[18].

RESULTS AND DISCUSSION

The numerical results are obtained for the RC(6)-08 airfoil at a freestream Mach number M_∞ of 0.3 and a chord Reynolds number Re of 10^5 and $3x10^5$ for the laminar Navier-Stokes code. In addition, the turbulent version of the code is evaluated at M_∞=0.35 and Re=$5.2x10^6$. The first part demonstrates the laminar flow modeling and the active control procedures. The second part demonstrates the turbulent flow modeling, a comparison with wind tunnel data and the active control procedures.

Active control is modeled by surface heating which modifies the temperature boundary condition over a small portion of the airfoil surface. The width of the control strip (h) is about 10 percent of the wavelength of the flow disturbance at the leading edge. The control temperature is modified according to the formula

$$\frac{T(t)}{T_{ref}} = \frac{T_w}{T_{ref}} + A + B^2 \sin f_n t \qquad (7)$$

In (7), T_w is the temperature of the wall (520 R°) and T_{ref} is the reference temperature (460 R°) where f, t, and n are the frequency, time, and an integer, respectively. The function models a D.C. and an A.C. current. The parameters of the heater for laminar flow are A=0.1 and B=1.22 for Re=10^5, and A=0.1 and B=0.87 for Re=$3x10^5$. For turbulent flow at Re=$5.2x10^6$, A=0.1

and B=0.61 are chosen. The maximum temperature of the heating strip is approximately 1.5 times the unheated absolute wall temperature. This temperature is lower than the temperature reported in the experiment[6] using tungston wire.

Accuracy of the computer solution and physical realism (i.e., flow patterns consistent with experimental observations) of the flow about the airfoil have been established by Rumsey and Thomas, including grid density and extent studies. In the present study, the grid refinement extending 10 chord lengths indicated that for laminar flow modeling a C-grid of 251x100 was sufficient while with turbulent flow modeling (up to 15 degrees angle of attack) a C-grid of 301x100 and 601x100 was used on a Cyber-205 computer and a Cray-2 computer respectively. The time step for the 301x100 grid was 0.001 and for the 601x100 grid was 0.0005.

LAMINAR FLOW AND CONTROL

The airfoil model is a helicopter blade section as depicted in Fig. 1. For laminar flow, consider first the freestream Mach number $M_\infty = 0.3$ and an angle of attack $\alpha=10°$. The separation region starts at the leading edge and continues downstream over the chord and into the wake region exerting large scale periodic oscillation.

Active control of the separation is accomplished by modulating the natural shedding frequency with surface heating. Tables 1 and 2 and Figs. 2 to 7 show the results of the uncontrolled and controlled cases. The steady state, the root mean square (RMS), and instantaneous lift and drag coefficients C_L, C_D, $\sqrt{\overline{C_L^2}}$, $\sqrt{\overline{C_D^2}}$, $C_L(t)$, and $C_D(t)$ show an increase in lift and reduction in drag for the control runs. Surface heating induces both local as well as global circulation about the upper surface. The global field is characterized by the vortices being shed periodically from the separation point at the leading edge. These vortices trigger large scale circulatory motion with clockwise rotation upstream of the trailing edge and with counterclockwise downstream. The separation point at the leading edge displays characteristic instability in the form of a sequence of discrete vortices consistent with experimental observations[7]. Using the conventional definition for Strouhal number $S(f)=(f\ c\ \sin\alpha)/U_\infty$ where U_∞ is the free stream velocity, the fundamental mode $S(f_1)$ is 0.13 and the first harmonic mode $S(f_2)$ is 0.26 (Table 1). These results are in close agreement with that for a Joukowski airfoil[19].

The normalized perturbation velocity at half chord is shown in figures 4 and 5. The maximum perturbation occurs at 2 percent of the chord in the vertical plane and its period is the same as the global period. The RMS increase due to surface heating is the difference between 0.307 and 0.449 and between 0.288 and 0.379 for the two Reynolds numbers. The strong coupling between surface heating and separated flow causes the shear layer to resonate through its harmonics inducing additional vortical motion that remains close to the airfoil. This feature contributes to an increase in lift. The normalized mean velocity profiles (Fig. 3) show a definite reduction in separation affecting all the upper surface. Furthermore, the pressure distribution (Fig. 6) shows the region in which control has been most effective over the airfoil. The functional form of the heat input is plotted in Fig. 7. The period matches that of vortex shedding. The summarized results in Table 2 demonstrate that localized surface heating has obvious attraction as a means for actively exciting the region of flow separation. Results confirm that an externally imposed temperature field increases the perturbation (as shown by the higher RMS value) within the separated layer and thus increases the compactness of the flow and reduces the separation.

TURBULENT FLOW AND CONTROL

This section is divided into two parts. The first part discusses the comparison of analysis with experiment for pressure distributions, lift coefficients and drag coefficients at different angles of attack at a Reynolds number of 5.2×10^6 and a Mach number of 0.35. In the second part, the effect of active control by surface heating is presented and discussed.

1. Comparison with Experiment

The comparison of lift and drag coefficients and pressure distributions from the Navier-Stokes code with wind tunnel measurements (unpublished data) is shown in Figs. 8 and 9. The experiment provides a broad range of conditions up to an angle of attack $\alpha=12.46°$. The major difference between the experiment and the numerical result is in the pressure distribution near the leading edge at high angles of attack. The lift coefficients increase linearly up to $\alpha \sim 8°$ and beyond that the coefficients exhibit a behavior resembling that of a stall of mixed type. The comparison of C_L and C_D are accurately predicted about the middle range of the angles of attack. The difficulty for the larger α condition where flow separates is in the resolution of the surface pressure since the perturbation field is a significant portion of the total signal. In addition, the experimental values of the maximum lift coefficients of an airfoil measured in the Langley 6- by 28-Inch Transonic Tunnel are known to be low (on the order of 0.10) due to the influence of the tunnel sidewall boundary layers.[21] The resolution at higher angles of attack in the presence of large separation needs further study both from the experimental and numerical points of view. From a numerical point of view, further grid resolution is needed at higher α. For the experiment, a real-time resolution from D.C. to higher frequencies is also needed.

2. Active Control

Results from the controlled and uncontrolled runs are shown in Figs. 10 through 16. The width of the control strip (h) is 2 percent of the airfoil chord and the strip is located near the leading edge Fig. 1. The control temperature T(t) reaches a peak at about 1.5 times the local steady ambient value. At the highest angle of attack, $\alpha=15°$, the computation is made with two different grid sizes 301x100, and 601x100, since it was found that grid refinement is needed for $\alpha>13°$ because of the separation which dominates over the upper surface.

The perturbation velocity at the half chord point at $\alpha=15°$ is lower closer to the surface and it increases with distance from the surface, an indication that the flow is separated over part of the layer. Surface heating activated near the leading edge augments the circulation over the upper surface thus reducing the separation significantly. This is observed by the increase in velocity perturbation. The improved circulation is also apparent by the mean velocity profile at three stations on the upper surface where the controlled profile has significantly reduced the region of separation as compared with the uncontrolled profile Fig. 11. The velocity perturbation is characterized by discrete harmonically related peaks with nondimensional frequency $fc/a_\infty=0.145$; 0.290; 0.445; 0.630; 0.760 and 0.950 at $y/c=10^{-2}$ and above while close to the surface only the odd harmonics are excited. The spectra of the velocity for the control case exceeds the amplitude of the uncontrolled one at all frequencies, especially with increased distance from the surface. For the control run, frequencies tuned to the naturally shedding frequencies are used to enhance receptivity. When the power spectral density of the longitudinal velocity for the controlled case is compared with the corresponding uncontrolled case, the effect of surface heating is clearly noticed. The coupling between surface heating and separated flow causes the shear layer to resonate through its harmonics, thus inducing additional vortical motion as observed in the experiments.[6,7]

The effect of control in the variation of C_L with α and C_D with C_L is to provide a significant increase in lift and reduction in drag, Figs. 14 and 15. The effect of grid size is also noticed for the higher α indicating an increase in grid resolution is needed with the increases in angle of attack.

The pressure coefficient time history is given in Fig. 16. The amplitude at three different nondimensional times (ta_∞/c)=10.00, 10.75, and 11.50, responds globally to the variation of the oscillating pressure about the airfoil. Regions of high pressure for the control run are maintained over the upper surface indicating a smaller separation than the uncontrolled run with lower pressure. This can also be noticed from the lift and drag coefficient time history Fig. 2 at lower Reynolds number illustrating that the uncontrolled runs maintain lower fluctuating lift and higher fluctuating drag over the cycle.

Control of the unsteady turbulent separation is not yet well understood in a fundamental sense. The numerical analysis of the flow field continues to search for an efficient code that can be used over broader ranges of practical situations.

The steady state compares with the experiment satisfactorily. The RC(6)-08 airfoil has good performance due to the extended unseparated region over the upper surface up to $\alpha \sim 8°$. It produces substantial high lift and low drag (at about 5 million Reynolds number, the upper limit of the present investigation). Active separation control works well on this airfoil since it delays massive separation and stall.

CONCLUDING REMARKS

The objective to show performance enhancement of an airfoil at high angle of attack was demonstrated at low and high Reynolds numbers by means of actively controlling the separation using localized surface heating. The results illustrate that the effect of control of separated flow is very much related to the wave form, the amplitude, and the bandwidth of the temperature function for a given pressure gradient.[6] The temperature function of the surface heating can restructure the lift and the drag of the airfoil profoundly. When both amplitude and temporal behavior are chosen for high receptivity, improved performance beyond the design limit can result. Previously, active surface heating has been shown experimentally to trigger harmonics and transition. Furthermore, it was observed that forced excitations induce instability and resonance and increase the entrainment in the early part of the shear layer, and as a result, the separated region was reduced. Further experimental and numerical work is needed to study three-dimensional effects on rectangular and nonrectangular configurations.

There are many other practical applications in which some form of coupling -- thermal, acoustic, or vortical exist to enhance circulation and performance. This study has proven heat addition to be a very effective method for actively perturbing the separated shear layer resulting in a significant increase in lift and reduction in drag.

REFERENCES

1. Flatt, J., "Boundary Layer and Flow Control," Vol. I, edited by Lachmann, G. V., Bergamon Press, Vol. I, 1961.

2. Holstein, H., "Messungen Zur Laminar Haltung der Grenzzchicht durch Absaugung an einem Trangflugel," Ber. S. Loder, Lilienthal Ges., P-17, 1942.

3. Reshotko, E., "Blowing and Suction in Viscous Flow Drag Reduction," ed. G. R. Hough, Prog. in Astro. & Aero., Vol. 72, AIAA, New York, p-185, 1980.

4. Lachmann, G. V., "Boundary Layer and Flow Control Its Principles and Application," Edited by G. V. Lachmann, Vol. 2, Pergman Press, 1961.

5. Liepmann, H. W., and Nosenchuck, D. M., "Active Control of Laminar-Turbulent Transition," Journal of Fluid Mechanics, Vol. 118, p. 201-204, 1982.

6. Maestrello, L., "Active Transition Fixing and Control of Boundary Layer in Air," AIAA Journal, Vol. 24, No. 10, p. 1577-1581, 1986.

7. Haung, L. S., Maestrello, L., and Bryant, T. D., "Separation Control Over an Airfoil of High Angle of Attack by Sound Emanating From the Surface," AIAA paper 87-1261, 1987.

8. Bayliss, A., Maestrello, L., Parikh, P., and Turkel, E., "Numerical Simulation of Boundary-Layer Excitation by Surface Heating/Cooling," AIAA Journal, Volume 24, No. 7, July 1986, p. 1095-1101.

9. Maestrello, L., Parikh, P., Bayliss, A., and Turkel, E., "Active Control of Compressible Flows on a Curved Surface," SAE 1985 Transactions, Volume 94, Section 6, 1986, p. 664-673.

10. Maestrello, L., Parikh, P., and Bayliss, A.," Instability and Sound Emission Over a Curved Surface," 1986 ASME Winter Annual Meeting, December 7-12, 1986, Anaheim, California. Proceedings pending.

11. Walsh, M. J., "Riblets as Viscous Drag Reduction Technique," AIAA Journal, Vol. 21, No. 4, p. 485, 1983.

12. Reshotko, E., "Control of Boundary Layer Transition," AIAA paper 85-0562, 1985.

13. Ahuja, K. K. and Burren, R. H., "Control of Flow Separation by Sound," AIAA paper 84-2298, October 1984.

14. Zaman, K. B. M. Q., Bar-Sever, A. and Mangalam, S. M., "Effect of Acoustic Excitation on the Flow Over a Low Reynolds Number Airfoil," Journal of Fluid Mechanics, Vol. 182, September 1987, pp. 127-148.

15. Sigurdson, L. W. and Roshko, A., "Controlled Unsteady Excitation of a Reattaching Flow," AIAA paper 85-0552, March 1985.

16. Arieli, R., Tauber, M. E., Saunders, D. A., and Caughey, D. A., "Computation of Transonic Flow About Helicopter Rotor Blades," AIAA Journal, Vol. 24, No. 5, p. 722-727, 1986.

17. McCroskey, W. J.," Some Current Research in Unsteady Fluid Dynamics - The 1976 Freeman Scholar Lecture," Transaction of the ASME, March 1977, pp. 8-34.

18. Rumsey, C. L., Anderson, W. K., "Some Numerical and Physical Aspects of Unsteady Navier-Stokes Computations Over Airfoils Using Dynamic Meshes," AIAA paper No. 88-0329.

19. Rumsey, C. L., Thomas, J. L., Warren, G. P., and Liu, G. C., "Upwind Navier-Stokes Solutions for Separated Periodic Flows," AIAA paper 86-0247, 1986.

20. Baldwin, B. S., and Lomax, H., "Thin Layer Approximation and Algebraic Model for Separated Turbulent Flows," AIAA paper 78-257, 1978.

21. Bingham, G. J. and Noonan, K. W., "Two-Dimensional Aerodynamic Characteristics of Three Rotorcraft Airfoils at Mach Numbers From 0.35 to 0.90," NASA TP 2000, May 1982.

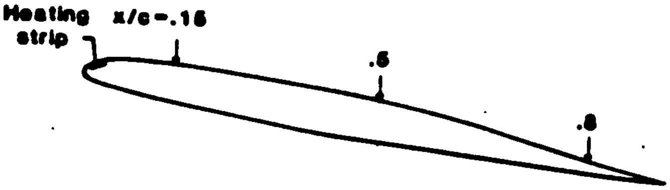

Figure 1. The RC(6)-08 airfoil.

	UNCONTROLLED					
Re	C_L	C_D	$S(f_1)$	$S(f_2)$	$\sqrt{\overline{C_L^2}}$	$\sqrt{\overline{C_D^2}}$
10^5	.5588	.1094	.13	-	.587	.118
3×10^5	.8211	.1703	.13	.26	.938	.179

Table 1. Uncontrolled laminar separation, $M_\infty = 0.3$, $\alpha = 10^0$.

	CONTROLLED				
Re	h/c	C_L	C_D	$\sqrt{\overline{C_L^2}}$	$\sqrt{\overline{C_D^2}}$
10^5	.04	.6900	.0594	.750	.061
3×10^5	.03	.9602	.1425	1.023	.147

Table 2. Controlled laminar separation, $M_\infty = 0.3$, $\alpha = 10^0$.

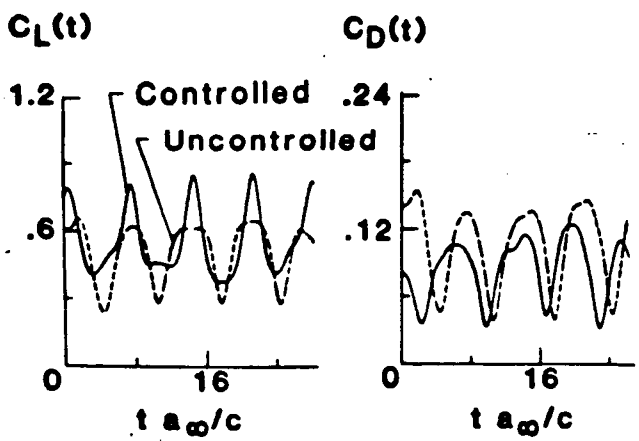

Figure 2. Global lift and drag coefficients $R_e = 10^5$, $M_\infty = 0.3$, $\alpha = 10°$.

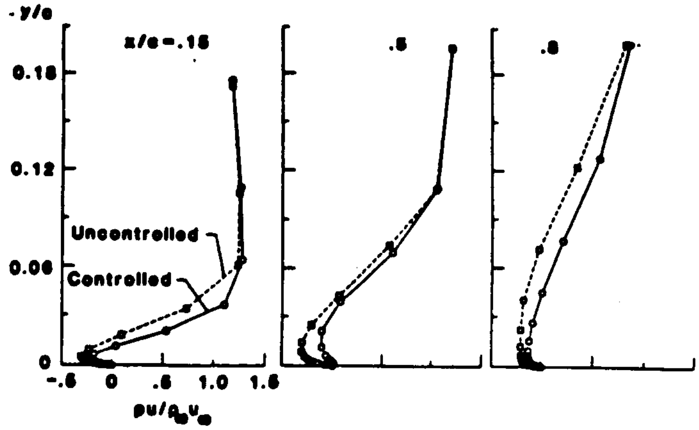

Figure 3. Mean velocity profile over the upper surface $R_e = 10^5$, $M_\infty = 0.3$, $\alpha = 10°$.

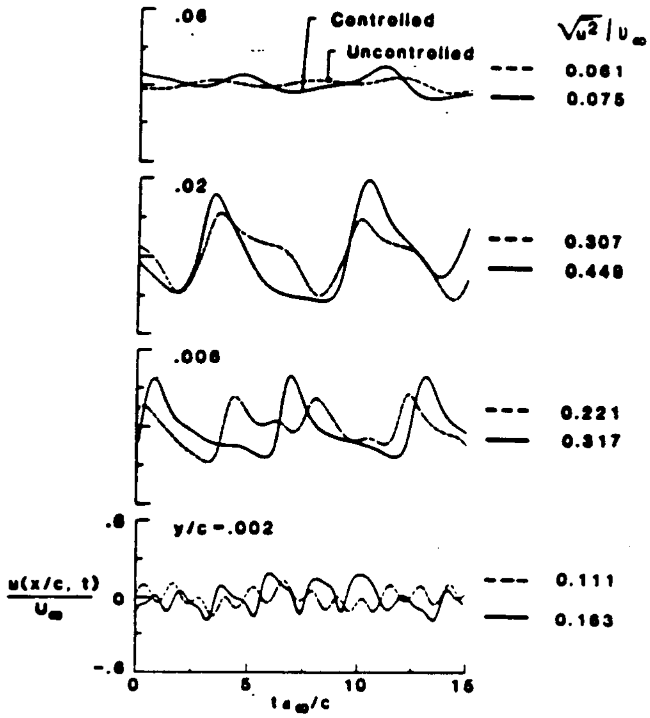

Figure 4. Velocity perturbation $R_e = 10^5$, $M_\infty = 0.3$, $\alpha = 10°$, x/c = 0.5.

ORIGINAL PAGE IS
OF POOR QUALITY

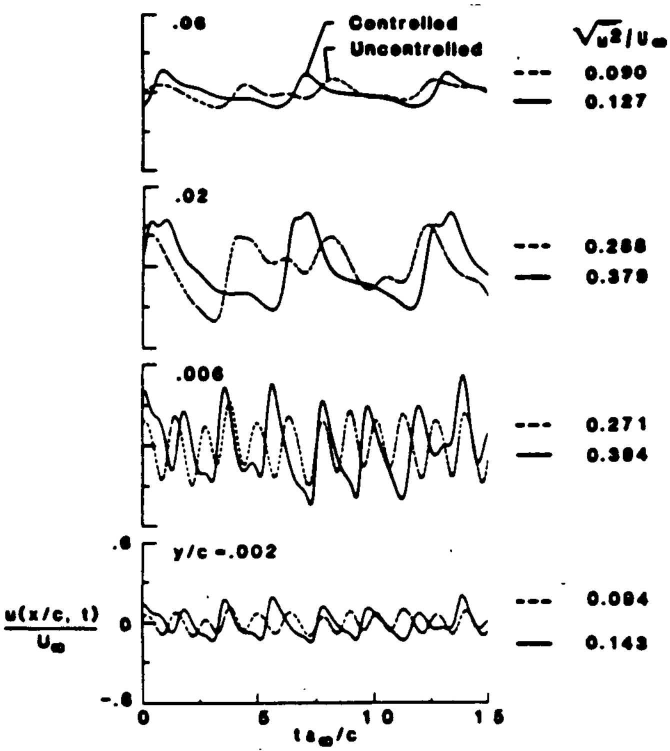

Figure 5. Velocity perturbation $R_e = 3 \times 10^5$, $M_\infty = 0.3$, $\alpha = 10°$, $x/c = 0.5$.

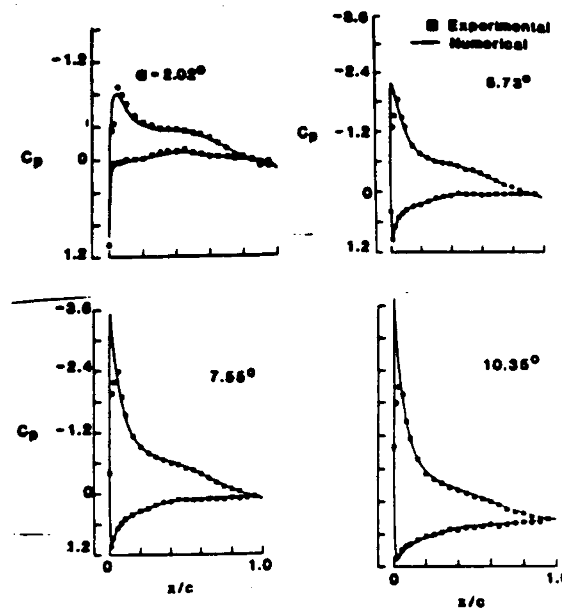

Figure 8. Pressure profile, $R_e = 5.2 \times 10^6$, $M_\infty = 0.35$.

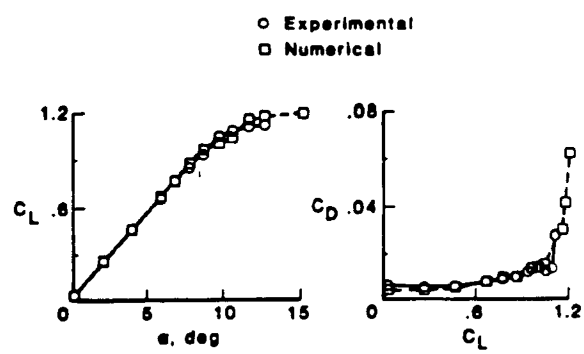

Figure 9. Lift and drag coefficients $R_e = 5.2 \times 10^6$, $M_\infty = 0.35$.

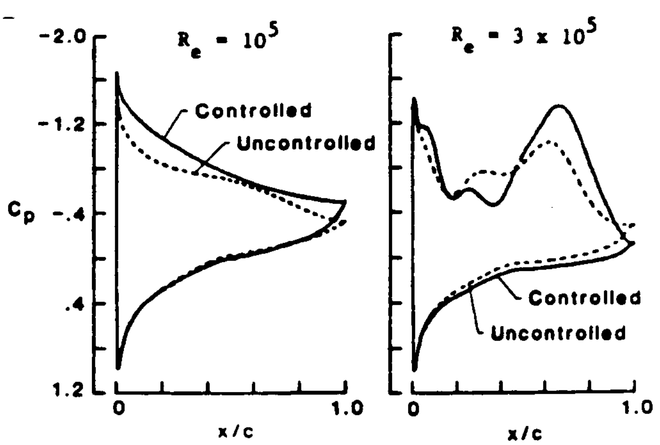

Figure 6. Pressure distribution, $M_\infty = 0.3$, $\alpha = 10^0$.

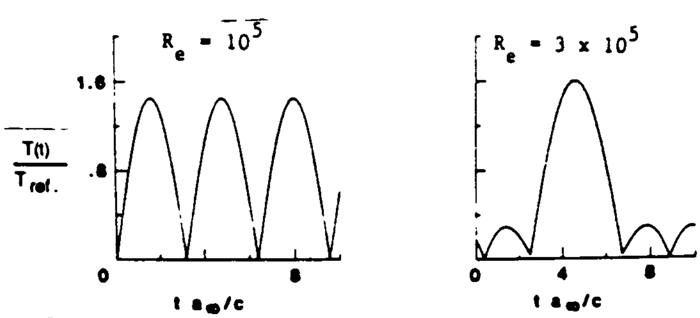

Figure 7. Control temperature function, $M_\infty = 0.3$, $\alpha = 10^0$.

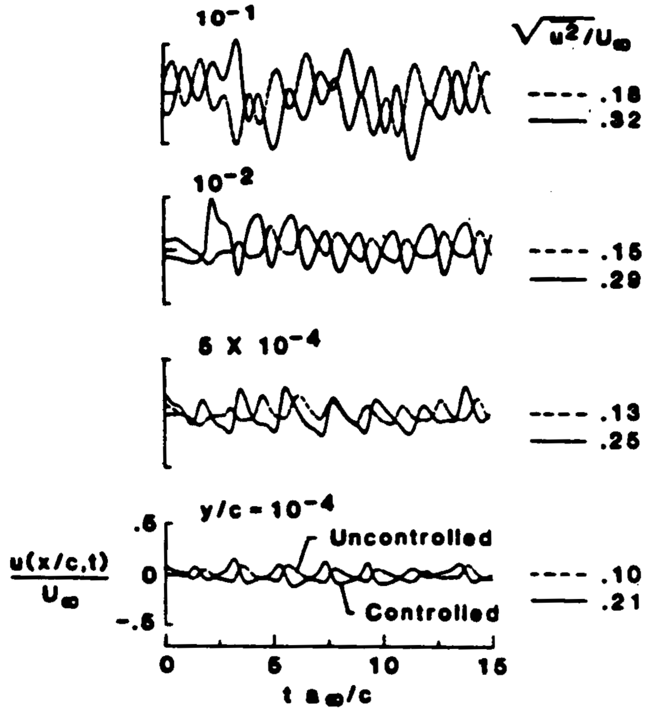

Figure 10. Velocity perturbation $R_e = 5.2 \times 10^6$, $M_\infty = 0.35$, $\alpha = 15°$, $x/c = 0.5$

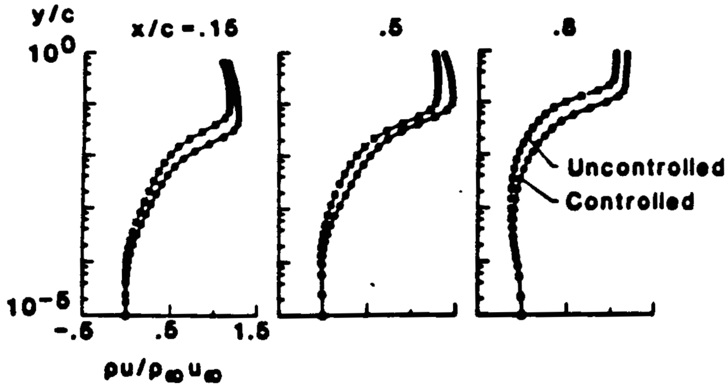

Figure 11. Mean velocity profile $R_e = 5.2 \times 10^6$, $M_\infty = 0.35$, $\alpha = 15°$.

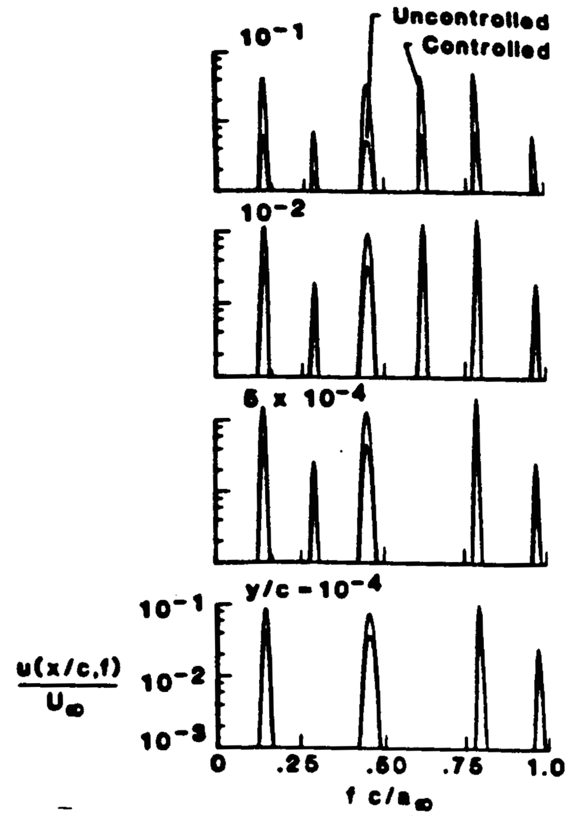

Figure 12. Power spectral density of the velocity $R_e = 5.2 \times 10^6$, $M_\infty = 0.35$, $\alpha = 15°$, $x/c = 0.5$.

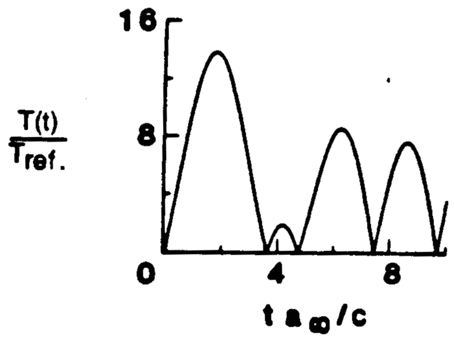

Figure 13. Control temperature function.

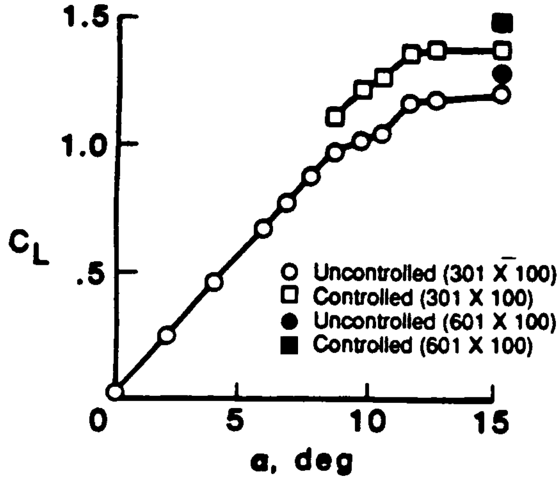

Figure 14. Lift coefficient.

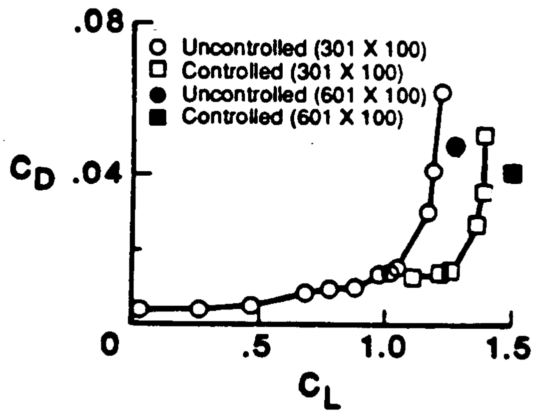

Figure 15. Drag coefficient.

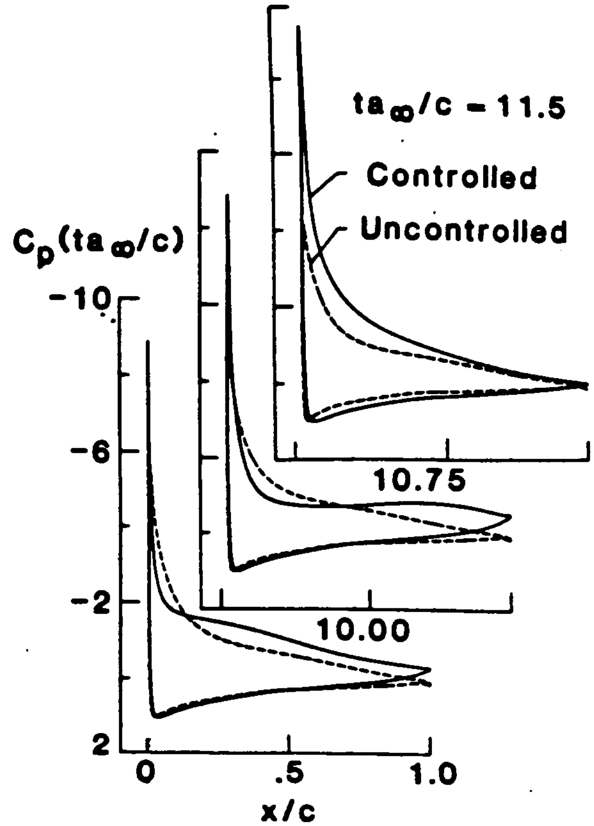

Figure 16. Instantaneous total pressure coefficient.

NASA
National Aeronautics and Space Administration

Report Documentation Page

1. Report No.	2. Government Accession No.	3. Recipient's Catalog No.
NASA TM-100563		

4. Title and Subtitle	5. Report Date
AN APPLICATION OF ACTIVE SURFACE HEATING FOR AUGMENTING LIFT AND REDUCING DRAG OF AN AIRFOIL	March 1988
	6. Performing Organization Code
7. Author(s)	8. Performing Organization Report No.
Lucio Maestrello, Forooz F. Badavi, and Kevin W. Noonan	
	10. Work Unit No.
	505-60-21
9. Performing Organization Name and Address	11. Contract or Grant No.
Langley Research Center National Aeronautics and Space Administration Hampton, Virginia 23665-5225	
	13. Type of Report and Period Covered
12. Sponsoring Agency Name and Address	Technical Memorandum
National Aeronautics and Space Administration Washington, D.C. 20546-0001	14. Sponsoring Agency Code

15. Supplementary Notes

Lucio Maestrello, Langley Research Center, Hampton, Virginia.
Forooz F. Badavi, PRC Kentron, Inc., Hampton, Virginia.
Kevin W. Noonan, Aerostructures Directorate, USAARTA-AVSCOM, Langley Research Center, Hampton, Virginia.

16. Abstract

Application of active control to separated flow on the RC(6)-08 airfoil at high angle of attack by localized surface heating is numerically simulated by integrating the compressible two-dimensional nonlinear Navier-Stokes equations solver. Active control is simulated by local modification of the temperature boundary condition over a narrow strip on the upper surface of the airfoil. Both mean and perturbed profiles are favorably altered when excited with the same natural frequency of the shear layer by moderate surface heating for both laminar and turbulent separation. The shear layer is found to be very sensitive to localized surface heating in the vicinity of the separation point. The excitation field at the surface sufficiently altered both the local as well as the global circulation to cause a significant increase in lift and reduction in drag.

17. Key Words (Suggested by Author(s))	18. Distribution Statement
Airfoils Flow control Lift augmentation	Unclassified--unlimited Subject Category 02

19. Security Classif. (of this report)	20. Security Classif. (of this page)	21. No. of pages	22. Price
Unclassified	Unclassified	16	A02

NASA FORM 1626 OCT 86